



## Article

# Analysis on the Effect of Obstruction on Sprinkler Skipping in Air Conditioner Room Fire

Ji Tae Kim <sup>1</sup>, Jun Suk Nam <sup>2</sup>, Ryang Hoon Kim <sup>1</sup>, Seung Yeon Kim <sup>3</sup> and Hong Sun Ryou <sup>1,\*</sup><sup>1</sup> School of Mechanical Engineering, Chung-Ang University, Seoul 156756, Korea<sup>2</sup> School of Fire Engineering, Gimcheon University, Gimcheon 39528, Korea<sup>3</sup> Fire Technology Research Center, Firebuster, Seoul 156756, Korea

\* Correspondence: cfdmec@cau.ac.kr; Tel.: +82-2-820-5280

**Abstract:** Sprinkler skipping is an important issue in fire spread. In general, two sprinklers are installed in air conditioner rooms at the ceiling and 30 cm below to avoid spray failure by energy recovery ventilator in the ceiling. However, there is a problem in that sprinkler skipping occurs in the air conditioner room. In this study, the sprinkler skipping phenomenon was analyzed through numerical analysis and the applicability of the open type of sprinkler operation method was reviewed. As a result, when the upper sprinkler works, sprinkler skipping occurred in all cases. The lower sprinkler shall not rise above the operating temperature of 68.3 °C with a maximum temperature of 65 °C. In particular, the spray failure caused by the energy recovery ventilator reduces the sprinkler head temperature by more than 8 °C by concentrating the spray droplets. As an open type, simultaneous operation of two sprinklers is capable of obtaining an appropriate fire extinguishing effect by covering the fire source with the spray of the lower sprinkler. The research results are expected to help in fire protection in buildings such as modern apartments with air-conditioned rooms.

**Keywords:** sprinkler skipping; air conditioner room; spray failure; temperature; apartments

**Citation:** Kim, J.T.; Nam, J.S.;

Kim, R.H.; Kim, S.Y.; Ryou, H.S.

Analysis on the Effect of Obstruction on Sprinkler Skipping in Air Conditioner Room Fire. *Energies* **2022**, *15*, 6776. <https://doi.org/10.3390/en15186776>

Academic Editor: Maria Founti

Received: 18 August 2022

Accepted: 5 September 2022

Published: 16 September 2022

**Publisher's Note:** MDPI stays neutral with regard to jurisdictional claims in published maps and institutional affiliations.



**Copyright:** © 2022 by the authors. Licensee MDPI, Basel, Switzerland. This article is an open access article distributed under the terms and conditions of the Creative Commons Attribution (CC BY) license (<https://creativecommons.org/licenses/by/4.0/>).

## 1. Introduction

The sprinkler system is the most used main system to prevent the spread of fire in buildings. Generally, sprinkler systems are installed on the final finished surface of the ceiling, but if the presence of an obstruction such as an energy recovery ventilator or duct in the ceiling has the potential to impede sprinkler spray, additional sprinklers must be added under the obstruction in the form of a pendant. However, if the upper sprinkler close to the ceiling operates first, the lower sprinkler which is mounted on the pendant of about 30 cm below the ceiling is cooling down by low temperature water droplet from the upper sprinkler. Therefore, the sprinkler skipping problem occurs by this effect of cooling down.

In general, sprinklers used in many buildings operate using a glass bulb that expands and breaks at a specific temperature as a trigger. Therefore, for the sprinkler to work, the glass bulb must receive sufficient heat from the surrounding environment. Ensuring sufficient spray density is particularly important to block convection and radiative heat transfer. Moreover, the sequential operation of sprinklers is an important factor in ensuring spray density. However, if the 'Sprinkler skipping' phenomenon occurs, there is a high possibility of problems in preventing and suppressing the spread of fire because sufficient spray density is not secured in the near of fire source. According to previous studies, there are four main mechanisms of sprinkler skipping: cooling by droplet, droplet impingement, water vapor condensation, and air entrainment by spray [1].

The following studies were conducted to investigate the heat transfer between the droplet and the flow and the cooling effect by the droplet impinging. The cooling effect was presented as an empirical formula by analyzing the temperature variation of sprinkler water temperature according to the droplet flux in a unit space [2–5]. As a result of this

study, it was shown that the droplet flux is about 80–125 g/m<sup>2</sup>s when water is discharging 1.9 L/s [1]. Additionally, by analyzing the heat transfer mechanism in droplet size distribution, temperature, and fire plume size, the relationship between sprinkler skipping occurrence ratio and heat release rate and temperature was presented.

Air entrainment is the air flow dragged by droplets that are sprayed from the ceiling to the floor. This air flow cools the sprinkler head and causes sprinkler skipping. Specifically, Heskestad et al. [4] showed that 0.85 m<sup>3</sup>/s of air entrainment in the ceiling layer was generated by a sprinkler with a flow rate of 1.9 L/s.

Based on this analysis, sprinkler design was performed to prevent sprinkler skipping. John L. DE RIS presented a theoretical concept for a skip-resistant sprinkler. This study provided a theoretical basis for the cooling of the incoming gas to the sprinkler based on the C-Factor of the sprinkler and the reduction of heat transfer by the shield [6]. Benjamin ditch et al. [7] experimented with sprinklers that added a shield to prevent water droplets from impinging. As a result, it was shown that an average maximum of 50% sprinkler skipping prevention effect can be seen when operating at 5.2 bar.

P. Croce et al. [8] presented a review paper on fast response sprinkler technology. The concepts of quick response residential sprinkler and early suppression fast response sprinkler have been summarized. In particular, early suppression fast response sprinkler was developed to deliver water quickly in the early stage of fire growth in an environment with rapid fire growth such as storage rack fire, but there is a high probability that sprinkler skipping will occur. If sprinkler spray is applied on the 12.2 m obstruction fire from the storage rack, the initial fire source suppression is slightly affected. However, the fire grew and strong plume carried the water droplets into the surrounding space, and the second ring sprinkler did not work, showing that sprinkler skipping occurred [9]. Therefore, in order to prevent such sprinkler skipping, FM Data sheets have been proposed through various studies and the NFPA 13 Standard has been proposed and continues to be studied [10]. Subsequently, complicate rules on an early suppression, fast-response sprinkler system installation method with regard to obstructions was proposed [8].

However, these sprinkler skipping studies are limitedly applicable only to an open space or a space similar to a storage rack, and the shape of obstruction. The reason for this limitation is that the flow caused by a fire should be differences depending on the shape of the space and the boundary of environmental conditions. In particular, in a narrow space, as an air conditioning room, which is recently constructed for aesthetics and safety reasons in high-rise buildings, the effects of space and obstruction should be considered together with the existing sprinkler skipping characteristics. Moreover, various obstructions such as ducts, pipes, and energy recovery ventilators are installed in the air conditioning room, and sprinklers are additionally installed under the obstructions. However, in case of fire, the sprinkler skipping phenomenon under the obstruction causes a lot of casualties.

Therefore, in this study, in order to prevent the sprinkler skipping phenomenon in air-conditioning rooms, the fire characteristics were analyzed by numerical method and the effectiveness of open-type simultaneous opening sprinklers was analyzed.

## 2. Numerical Setups

### 2.1. Governing Equations

Fire dynamic simulator (FDS), an open source program, was used to numerically analyze the behavior of fire and sprinklers. The detailed setup and governing equations of FDS are as follows [11].

### 2.1.1. Fluid Domain

We calculated the density, momentum, mass fraction of each species, and energy by four equations. Low Mach number Navier–Stokes equations were used to calculate the momentum and the turbulent model was selected for Large Eddy Simulation (LES) [11].

$$\frac{\partial \bar{\rho}}{\partial t} + \frac{\partial \bar{\rho} \tilde{u}_j}{\partial x_j} = \dot{m}_b'' \quad (1)$$

$$\bar{\rho} \left( \frac{\partial \tilde{u}_i}{\partial t} + \frac{\partial \tilde{u}_i \tilde{u}_j}{\partial x_j} \right) = -\frac{\partial \bar{p}}{\partial x_i} + \bar{\rho} g + f_i + \frac{\partial \tau_{ij}}{\partial x_j} \quad (2)$$

$$\frac{\partial (\bar{\rho} \tilde{Y}_l)}{\partial t} + \frac{\partial (\bar{\rho} \tilde{u}_j \tilde{Y}_l)}{\partial x_j} = -\frac{\partial}{\partial x_j} (\overline{\rho u_j Y_l} - \bar{\rho} \tilde{u}_j \tilde{Y}_l) + \frac{\partial}{\partial x_j} \left( \overline{\rho D_l \frac{\partial Y_l}{\partial x_j}} \right) + \bar{w}_l \quad (3)$$

$$\frac{\partial (\bar{\rho} \tilde{h})}{\partial t} + \frac{\partial (\bar{\rho} \tilde{u}_j \tilde{h})}{\partial x_j} = \frac{D \bar{p}}{Dt} + \frac{\partial}{\partial x_j} \left( k \frac{\partial \tilde{T}}{\partial x_j} - q_j^r \right) + \sum_l \frac{\partial}{\partial x_j} \left( \bar{\rho} D_l \tilde{h}_l \frac{\partial \tilde{Y}_l}{\partial x_j} \right). \quad (4)$$

### 2.1.2. Sprinkler

We have to calculate and the force  $f$  in the Equation (2), which is the momentum transferred from the droplets to the air.  $f$  This is calculated by

$$f = \frac{1}{2} \frac{\sum \rho C_D \pi r_d^2 (\mathbf{u}_d - \mathbf{u}) |\mathbf{u}_d - \mathbf{u}|}{\delta x \delta y \delta z} \quad (5)$$

We can calculate the following equation to analyze the trajectory of the droplets as written in Equation (6). Additionally, the equation of drag coefficient is determined according to the local Reynolds number Equations (7) and (8)

$$\frac{d}{dt} (m_d \vec{\mathbf{u}}_d) = m_d g - \frac{1}{2} \rho C_D \pi r_d^2 (\mathbf{u}_d - \mathbf{u}) |\mathbf{u}_d - \mathbf{u}| \quad (6)$$

$$Re = \frac{\rho |\mathbf{u}_d - \mathbf{u}| 2r_d}{\mu} \quad (7)$$

$$C_D = \begin{cases} 24/Re & Re < 1 \\ 24(1 + 0.15 Re^{0.687})/Re & 1 < Re < 1000 \\ 0.441000 < Re & \end{cases} \quad (8)$$

The mass loss rate of the droplet in the air is calculated by the following equations:

$$\frac{dm_d}{dt} = -2\pi r_d Sh \rho D (Y_d - Y_g) \quad (9)$$

$$Sh = 2 + 0.6Re^{\frac{1}{2}} + Sc^{\frac{1}{3}} \quad (10)$$

We have to calculate not only mass transfer but also energy transfer by the evaporation of the water droplets. The temperature of droplets is determined by the convective heat transfer across the surface of the droplets and the evaporation energy of water.

$$m_d c_{p,w} \frac{dT_d}{dt} = A_d h_d (T_g - T_d) - \frac{dm_d}{dt} h_v \quad (11)$$

The first term in the right hand side (RHS) means the convective heat transfer across the surface of the droplets, and the second term is the evaporation energy.  $h_d$  Equation (11) shows the heat transfer coefficient, which is calculated by

$$h_d = \frac{Nuk}{2r_d} \quad (12)$$

$$Nu = 2 + 0.6Re^{\frac{1}{2}}Pr^{\frac{1}{3}} \quad (13)$$

The real water droplet has various shapes; however, it was assumed to be spherical. The size distribution of water droplets can be specified in terms of Cumulative Volume Fraction (CVF), a function that indicates the fraction of the total mass carried by droplets less than the given diameter. The CVF for a sprinkler may be represented by a combination of log-normal and Rosin–Rammer distributions [12]:

$$\frac{1}{\sqrt{2\pi}} \int_0^D \frac{1}{\sigma D} \exp\left(-\frac{[\ln(\frac{D}{D_{v,0.5}})]^2}{2\sigma^2}\right) dD \quad (D \leq D_{v,0.5})$$

$$1 - \exp\left[-0.693\left(\frac{D}{D_{v,0.5}}\right)^\gamma\right] \quad (D > D_{v,0.5}) \quad (14)$$

where  $D_{v,0.5}$  is the median volumetric droplet diameter (i.e., half the mass is carried by droplets with diameters of  $D_{v,0.5}$  or less),  $\gamma$  and  $\sigma$  are empirical constants equal to approximately 2.4 and 0.48, respectively [12]. The median droplet diameter  $D_{v,0.5}$ , was estimated using the formula reported by Yu [13]:

$$\frac{D_{v,0.5}}{D} = C_{sp} W_e^{-1/3} \quad (15)$$

$$W_e = \frac{\rho_d u_d^2 D}{\sigma_d} \quad (16)$$

where  $D$  is the orifice diameter of the sprinkler.  $\rho_d$  is the density of water in  $\text{kg/m}^3$ ,  $u_d$  is the initial droplet velocity in  $\text{m/s}$ , and  $\sigma_d$  is the water surface tension in  $\text{N/m}$ . Analysis of Sheppard's data results in an average value of  $C_{sp}$  approximately 1.53 for sprinklers tested [14].

## 2.2. Geometry and Mesh Generation

In this study, we set two types of geometry, which is with and without an energy recovery ventilator in order to study on the problem of sprinkler's skipping. In Figure 1, we described the geometry without the energy recovery ventilator. It is necessary to set two sprinklers to study on the skipping phenomenon. The upper and lower sprinklers are located 0.2 m and 0.5 m down from the ceiling, respectively. The upper sprinkler ejects in an upward direction, but the lower sprinkler ejects in a downward direction. In high-rise buildings, air-conditioning rooms are being constructed for safety and aesthetic reasons, and the geometry of the air-conditioning rooms is the average of three recently constructed high-rise apartment buildings. The size of the air conditioner is  $0.6 \times 0.2 \times 0.5 \text{ m}^3$  and the room is  $1.8 \times 1.8 \times 2.75 \text{ m}^3$ . The air conditioner is located on the floor 0.1 m away from the louver. In Figure 1e, we drew the geometry with the energy recovery ventilator. Every condition was the same as the geometry described in Figure 1, but an energy recovery ventilator exists in this geometry. The size of the energy recovery ventilator is  $1.5 \times 0.5 \times 0.4 \text{ m}^3$  and located 0.4 m away from left wall, opposite to louver. We set 236,000 hexahedral meshes which size of mesh as  $0.1067 \times 0.1033 \times 0.1050 \text{ m}^3$  through grid independence test.

## 2.3. Numerical Setup

Numerical analysis was performed on three cases as shown in Table 1. The first case is a case where two sprinklers are installed 20 cm and 50 cm below the ceiling in the

absence of an obstruction such as energy recovery ventilation. Additionally, the energy recovery ventilator was set to inactive so that it did not generate flow or heat. Case 2 added obstruction from Case 1. Case 3 is a case where there is obstruction and two sprinklers were operated at the same time.

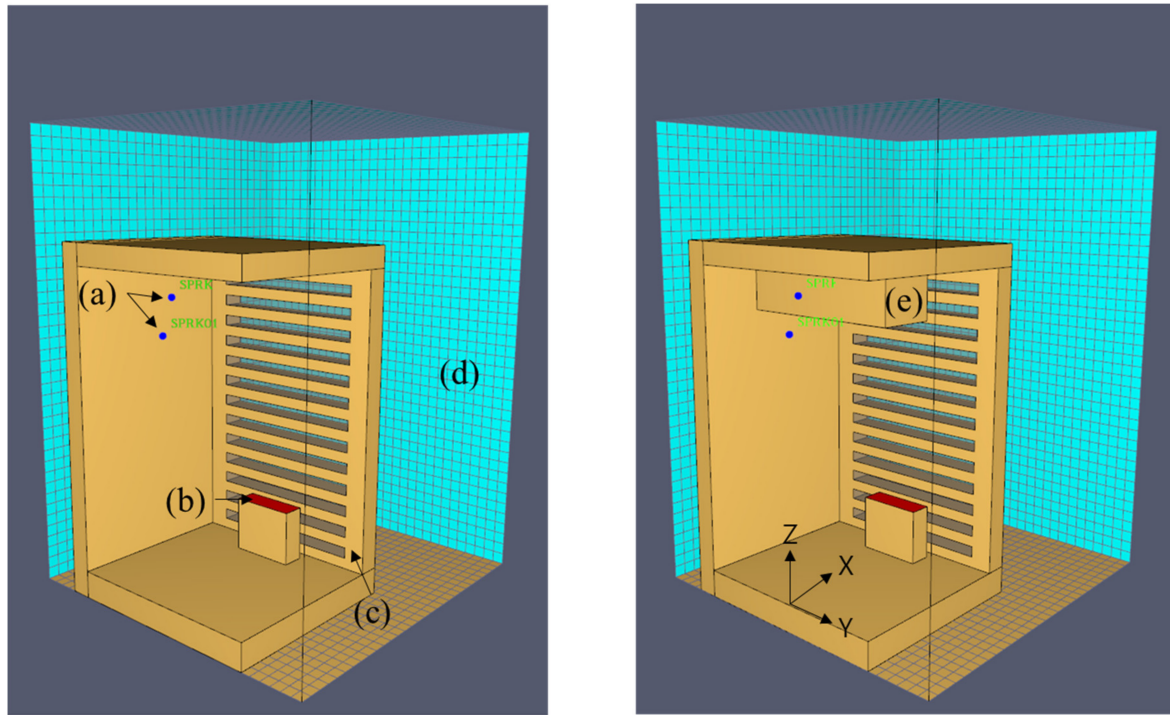


**Figure 1.** Geometry of the enclosure room fire, (a) sprinkler: sprinklers are installed 20 and 50 cm under the ceiling, (b) fire source, (c) louver, (d) open boundary, (e) obstruction.

**Table 1.** Summary of numerical cases.

Cases	Obstruction	Sprinkler Operation Type	Fire Source	Louver
Case 1	X	Closed	90 kW 600 s	Open
Case 2	O	Closed	90 kW 600 s	Open
Case 3	O	Open	90 kW 600 s	Open

### 2.3.1. Fire Source and Heat Release Rate

Heat release rate (HRR) is the most important parameter to simulate a fire, because it represents the growth of a fire. For the fire growth curve, a  $t^2$  curve was used that expresses the combustion characteristics according to the material of the fire source in a lumpy manner [12]. The fire source was assumed to be an air conditioner outdoor unit. Through the previous experimental study [15], we set the maximum value of HRR as 90 kW and the ramp-up time as 600 s.

### 2.3.2. Sprinkler

The two sprinklers set in this study have the same mass flow rate about 80 L/min. Their jet stream types are conical and have same velocity, 5 m/s. In addition, their jet stream offset is 0.05 m from sprinkler outlet, and two latitude angles are 60 and 75 degrees, respectively. The shape of water particle was set to sphere, and dense volume fraction was set to  $1.0 \times 10^{-5}$ . The activation temperature of upper and down sprinkler are 68.33 °C and response time index are  $50 \sqrt{\text{ms}}$ .

### 2.3.3. Boundary Conditions

We assumed that a fire occurs on only the top surface of the air conditioner. So, the fire source was set as a burner with Heat Release Rate Per Unit Area (HRRPUA) in units of  $\text{kW}/\text{m}^2$ . Five walls of the room are inert, and the other one wall is a louver. We set the pressure 0 Pa, so the air freely enters and exits through this louver. If there is no air domain outside the room, the boundary condition of 0 Pa could affect the results of simulation. Thus, we additionally made the air domain. The left and bottom walls of the air are inert, and the others are open. The air flows in and out through these open walls.

## 3. Results

### 3.1. Effect of Obstruction in Sprinkler Spray Pattern

The change of sprinkler spray pattern according to the presence of obstruction was analyzed as shown in the Figure 2. Blue and red particles represent water droplets sprayed from sprinklers installed 0.2 and 0.5 m below the ceiling respectively. The time the analysis was performed was 600 s when 100 s after the sprinkler was operated.

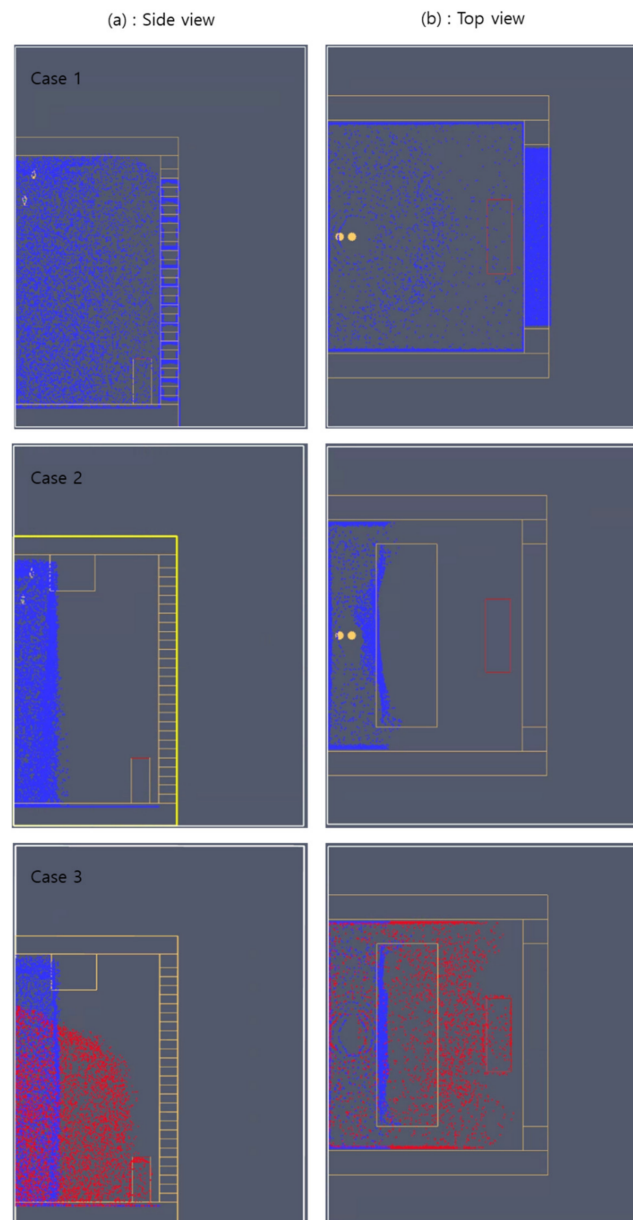


**Figure 2.** Sprinkler spray pattern according to the obstruction, (a): Side view, (b): Top view.

In Case 1, the blue droplet sprayed from the upper sprinkler was relatively evenly distributed in the air-conditioned room, but there was no red droplet from the lower sprinkler. The upper sprinkler was operated by a fire source, but the lower sprinkler did not work, causing a sprinkler skipping phenomenon. An analysis of the effect of temperature on lower sprinkler operation is detailed in the next chapter. Additionally, the droplets sprayed from the upper sprinkler show the trend of spraying most of the enclosure space in a circular shape as shown in the Figure 2b side view. Moreover, some of the sprayed droplets show movement toward the louver exit.

Case 2 shows a spray pattern in which droplets sprayed from the upper sprinkler are blocked by obstruction. Since the spray flow is not formed at all toward the fire source due to the spray failure caused by the obstruction, it is considered that there are many problems in suppressing the fire source even if the propagation of the fire to the obstruction can be prevented.

Case 3 is a spray pattern of a system in which the upper sprinkler is activated, and the lower sprinkler is also activated at the same time. The red droplet of the lower sprinkler has insufficient flow to the ceiling side close to the louver, but it shows a trend of sufficiently flowing as a fire source.

### 3.2. Effect of Obstruction in Temperature

In general, sprinklers operate by breaking glass bulbs by thermal expansion. Therefore, the analysis of the hot combustion gas is important for understanding the sprinkler skipping phenomenon. The temperature contour of XZ plan  $Y = 0$  is represent in Figure 3 at 600 s. The high-temperature combustion gas rises by the buoyancy flow generated by the fire, and the outside air is entrained under the louver as shown in the Figure 3a.

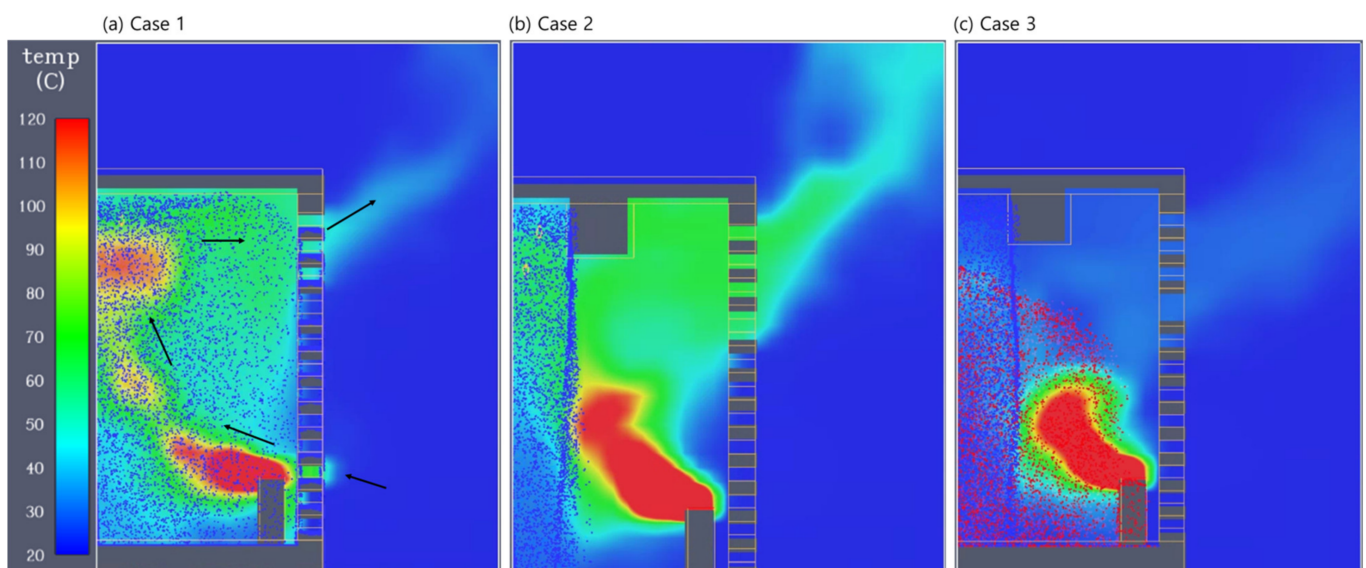


**Figure 3.** Temperature contour of XZ plan  $Y = 0$ , (a): Case 1, (b): Case 2, (c): Case 3.

In Case 1, since there is no obstruction, the water droplet is sprayed relatively evenly into the space, and the flow temperature discharged to the louver showed about 40–50 °C, which is relatively lower than that of Case 2. In addition, although the flow temperature around the lower sprinkler showed a relatively high trend; since the water droplets were impinged, the lower sprinkler head was sufficiently cooled to cause sprinkler skipping. The detailed temperature change over time of the sprinkler head is analyzed in the next chapter.

In Case 2 and Case 3, the spray flow of the upper sprinkler was blocked by the obstruction. Therefore, spray pattern of water droplets was concentrated under the obstruction. Therefore, the cooling effect of the flow around the lower sprinkler further increased, and

the maximum temperature was maintained below  $62\text{ }^{\circ}\text{C}$ , which has a more adverse effect on the sprinkler skipping.

Case 3 had the lowest overall temperature distribution because both sprinklers were operating. In Case 3, as described above, when the upper sprinkler works, the lower sprinkler is also set to work. Thus, it works freely with sprinkler skipping. Droplets sprayed from the lower sprinkler were properly sprayed near the fire source; therefore, the overall temperature of the space showed the lowest trend.

The velocity contour of XZ plan  $Y = 0$  is represented in Figure 4 at 600 s. In all cases, the flow is caused by buoyancy, and after impinging the ceiling, a ceiling jet with a maximum flow velocity of  $2\text{ m/s}$  is formed in the direction of the louver. In Case 1, it was formed near the ceiling because there is no obstruction that prevents the flow of the ceiling jet. However, the flows of Case 2 and Case 3 showed downward trends under obstruction. In addition, the flow velocity after exiting the louver was the fastest in Case 2. After exiting the louver, the flow velocity of the flow was most affected by the buoyancy force.

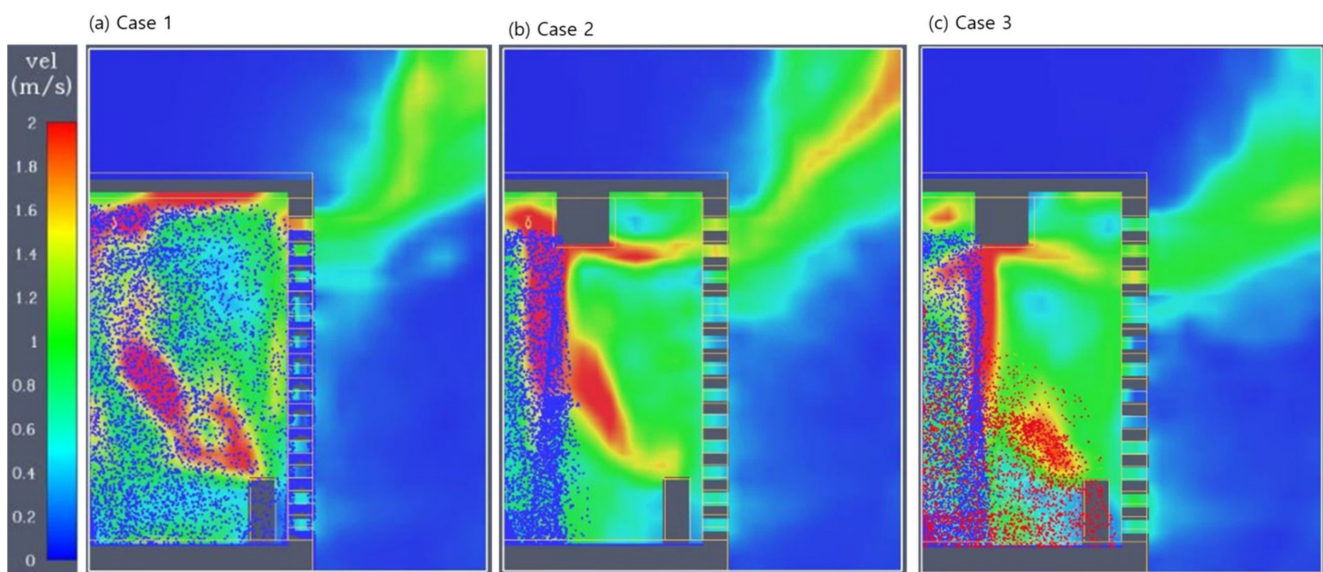


**Figure 4.** Velocity contour of XZ plan  $Y = 0$ , (a): Case 1, (b): Case 2, (c): Case 3.

The temperature of the flow exiting through the louver near the ceiling was the highest in Case 2 as shown in the Figure 5. This variation in temperature is due to the cooling effect of water droplets as described in Figure 3 above. Moreover, there was relatively high fluctuation in temperature because the velocity of Case 2 was relatively higher than other cases.

The sprinkler head temperatures for each case are shown in Figure 6. Obstruction delays the upper sprinkler head activation time by about 15 s to block the flow of high-temperature combustion gas about 540 s, 555 s, and 555 s in Case 1, Case 2, and Case 3 respectively. The increasing rate of the lower sprinkler temperature is relatively low because the combustion gases need to come down 50 cm from the ceiling. The maximum temperatures of the lower sprinkler were  $65\text{ }^{\circ}\text{C}$ ,  $57\text{ }^{\circ}\text{C}$ , and  $57\text{ }^{\circ}\text{C}$  in Case 1, Case 2, and Case 3 respectively, lower than the sprinkler operating temperature of  $68.33\text{ }^{\circ}\text{C}$ .

In particular, after the upper sprinkler operation, the lower sprinkler head temperature of case 1 shows a trend of continuously increasing unlike other cases. This change in the sprinkler head temperature in case 1 is thought to be related to the spray pattern. As explained in the previous chapter, the temperature variation of the sprinkler head is affected by the high-temperature flow from fire source and the cooling effect by sprinkler spray. In Case 2 and Case 3, the spray patterns of the upper sprinkler were concentrated downward due to obstruction, and the water droplet densities were increased, resulting in



sufficient cooling, and limiting the temperature rise. However, in case 1, it was analyzed that the temperature rose because the water droplet density was low.

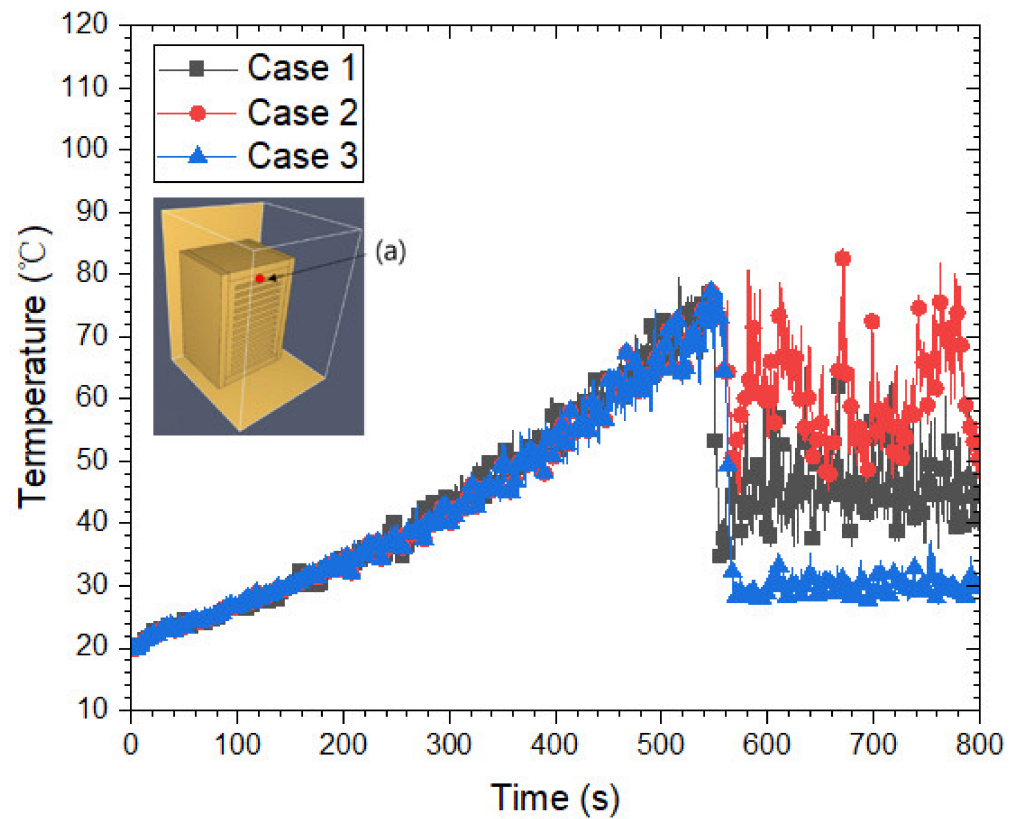


Figure 5. Temperature variation at the louver, (a): measurement point.

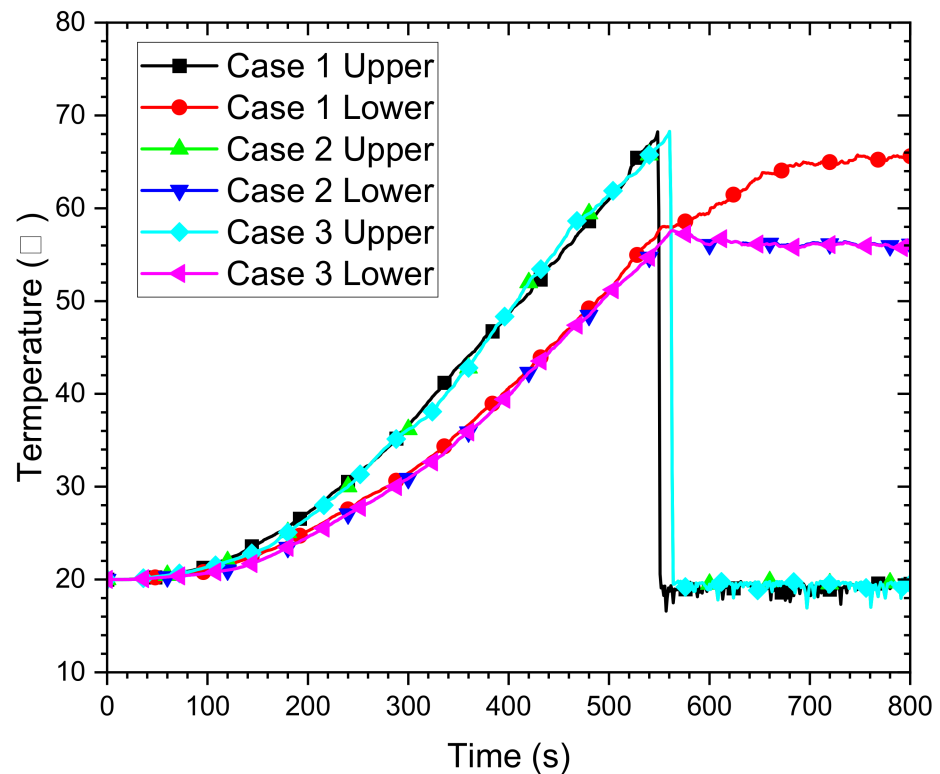


Figure 6. Temperature variation at the sprinkler head.

#### 4. Conclusions

The sprinkler skipping phenomenon that occurs in the case of a condenser fire in an air-conditioned room was analyzed by a numerical method. In general, two sprinklers were installed in air conditioner room at ceiling and 30 cm below to avoid spray failure by obstruction as duct and energy recovery ventilator in ceiling. However, the sprinkler skipping phenomenon occurred under all operating conditions, where the high-temperature heat flow from the fire source only operated the upper sprinkler close to the ceiling. In particular, the maximum temperature of the lower sprinkler was 65 °C, which is lower than the sprinkler operating temperature of 68.33 °C. The reason for this is that the water droplets sprayed from the upper sprinkler are sufficiently cooled by the flow temperature in the space, impinging on the sprinkler head. This is because the water droplet sprayed from the sprinkler sufficiently cools the flow in the space, and the low-temperature water droplet is impinged into the sprinkler head. Sprinkler skipping is exacerbated because the spray is blocked by obstruction. Moreover, it is analyzed that spray failure due to obstruction will be a problem because water droplets are not sprayed to the fire source.

Therefore, as an open type, simultaneous operation of two sprinklers could be able to obtain an appropriate fire extinguishing effect by covering the fire source with the spray of the lower sprinkler. This research results are expected to help in fire protection in buildings such as modern apartments with air-conditioned rooms. In addition, the results of this study can be usefully applied not only to air-conditioned rooms, but also to underground parking lots where sprinkler spray is disturbed by ducts and pipes.

**Author Contributions:** Funding acquisition, J.S.N. and S.Y.K.; Investigation, R.H.K.; Writing—original draft, J.T.K.; Writing—review & editing, H.S.R. All authors have read and agreed to the published version of the manuscript.

**Funding:** This work was supported by the Technology development Program S3035584 funded by the Ministry of SMEs and Startups (MSS, Korea), also this work supported by the Gimcheon university.

**Institutional Review Board Statement:** Not applicable.

**Informed Consent Statement:** Not applicable.

**Conflicts of Interest:** The authors declare no conflict of interest.

#### Nomenclature

$u_j$	velocity	$q_j^r$	radiative heat transfer
$\dot{m}_b''$	mass source term	$m_d$	mass of the droplet
$p$	pressure	$\mathbf{u}_d$	velocity vector of the droplet
$g$	gravity	$r_d$	droplet radius
$f_i$	body force	$C_D$	drag coefficient
$Y_l$	mass fraction for species $l$	$Re$	Reynolds number
$D$	droplet diameter	$Y_d$	mass fraction of the droplet
$D_l$	diffusivity for species $l$	$Y_g$	mass fraction of the gas
$w_l$	rate of reaction	$Sh$	droplet Sherwood number
$h$	enthalpy	$Sc$	Schmidt number
$T$	temperature	Greek letters	
$c_{p,w}$	specific heat of water	$\rho$	density
$T_d$	temperature of the droplet	$\tau_{ij}$	shear stress
$A_d$	surface area of the droplet	$\delta x \delta y \delta z$	volume of the grid cell
$h_d$	heat transfer coefficient	$\mu$	dynamic viscosity of air
$T_g$	temperature of the gas	Superscripts and subscripts	
$h_v$	heat of vaporization	$d$	droplet
$Nu$	Nusselt number	$w$	water
$k$	thermal conductivity of air	$g$	gas
$Pr$	Prandtl number	$v$	vaporization

## References

1. Croce, P.A.; Hill, J.P.; Xin, Y. An investigation of the causative mechanism of sprinkler skipping. *J. Fire Prot. Eng.* **2005**, *15*, 107–136. [[CrossRef](#)]
2. Dundas, P. *The Scaling of Sprinkler Discharge: Prediction of Drop Size*; Technical Report Optimization of Sprinkler Fire Protection; FMRC Serial; Factory Mutual Research Corporation: Norwood, MA, USA, 1974.
3. Heskestad, G. *Similarity Relations for the Initial Convective Flow Generated by Fire*; ASME Paper; ASME: New York, NY, USA, 1972; Volume 72, pp. 1113–1116.
4. Heskestad, G.; Kung, H.; Todtenkopf, N. *Air Entrainment into Water Sprays*; Factory Mutual System; FM Research; Factory Mutual Research Corporation: Norwood, MA, USA, 1981.
5. Dundas, P. *Cooling and Penetration Study*; FMRC Serial; Factory Mutual Research Corporation: Norwood, MA, USA, 1974.
6. De Ris, L.J.; Ditch, B.; Yu, H.-Z. The Skip-resistant Sprinkler Concept—Theoretical Evaluation. *J. Fire Prot. Eng.* **2009**, *19*, 275–289. [[CrossRef](#)]
7. Ditch, B.; De Ris, J.L.; Yu, H.-Z. The Skip-resistant Sprinkler Concept—An Experimental Evaluation. *J. Fire Prot. Eng.* **2009**, *19*, 291–308. [[CrossRef](#)]
8. Croce, P.; Beyler, C.; Dubai, C.; Johnson, P.; McNamee, M. Fast-Response Sprinkler Technology: Hsiang-Cheng Kung, Gunnar Heskestad, Robert Bill, Roger Allard: The 2019 Phillip J. DiNenno Prize. *Fire Technol.* **2020**, *56*, 1981–2001. [[CrossRef](#)]
9. Palenske, G.A.; Ornelas, G.N. Obstructions and Early Suppression Fast Response Sprinklers. *Fire Technol.* **2022**, 1–28. [[CrossRef](#)]
10. Mayer, N.; Parisian, K.; Gleason, A. *NFPA 13 Standard for the Installation of Sprinkler Systems*; National Fire Protection Association: Quincy, MA, USA, 2010.
11. McGrattan, K.; Hostikka, S.; McDermott, R.; Floyd, J.; Weinschenk, C.; Overholt, K. *Fire Dynamics Simulator Technical Reference Guide Volume 1: Mathematical Model*; NIST Special Publication; NIST: Gaithersburg, MD, USA, 2013; Volume 1018, p. 175.
12. McGrattan, K.; Hostikka, S.; McDermott, R.; Floyd, J.; Weinschenk, C.; Overholt, K. *Fire dynamics Simulator User's Guide*; NIST Special Publication; NIST: Gaithersburg, MD, USA, 2013; Volume 1019, pp. 1–339.
13. Yu, H. Investigation of spray patterns of selected sprinklers with the FMRC drop size measuring system. In Proceedings of the First International Symposium on Fire Safety Science, Gaithersburg, MD, USA, 7–11 October 1985.
14. Sheppard, D.T. *Spray Characteristics of Fire Sprinklers*; Northwestern University: Evanston, IL, USA, 2002.
15. Min, S.-H.; Bae, Y.-J. A Study on Combustion Experiments of Multi Type Air-Conditioner Outdoor Units by Large Scale Calorimeter. *Fire Sci. Eng.* **2011**, *25*, 168–177.